Anisotropic etching of RuO_2 and Ru with high aspect ratio for gigabit dynamic random access memory

Takashi Yunogami[a] and Kazuo Nojiri

Device Development Center, Hitachi, Ltd., 6-16-3, Shinmachi, Ome-shi, Tokyo 198-8512, Japan

Anisotropic RuO_2 and Ru etching technology for gigabit dynamic random access memory has been developed using high density $O_2 + 10\%$ Cl_2 plasma in an inductively coupled plasma etching system. Under the conditions of low pressure, high gas flow rate, and large overetching times, we have demonstrated 0.2 μm wide patterns in 0.3-μm-thick RuO_2/Ru films and 0.1 μm wide patterns in 0.45-μm-thick Ru films, both with an almost perpendicular taper angle of 89°. © *2000 American Vacuum Society.* [S0734-211X(00)01604-8]

I. INTRODUCTION

Recently, gigabit dynamic random access memory (DRAM) capacitors have been developed using simple stacked structures of high dielectric constant materials, such as barium strontium titanium oxide (BST).[1] Noble metals, such as Pt and Ru, or conductive oxides, such as RuO_2, have been used as electrode materials[2] since they are thermally stable in the high temperature oxygen ambient used for BST deposition. Very high resolution and aspect ratios are needed for the bottom electrode in these structures; the film thickness required for 0.13 μm critical dimensions (CDs) is 0.45 μm, implying an aspect ratio of 3.5:1. The angle of the sidewall taper must be larger than 85°.

It is difficult to achieve the required anisotropic profiles for Pt[3,4] by dry etching because the vapor pressure of the possible reaction products is low.[5] On the other hand, anisotropic etching of Ru and RuO_2 are possible[6,7] by oxygen ion assisted etching through the formation of volatile RuO_3 and RuO_4.[8] The addition of 10% Cl_2 to an O_2 plasma enhances this etch rate[9] further, because 10% Cl_2 increases the concentration of oxygen radicals and ions. In spite of these advances, the etching of Ru or RuO_2 with the required aspect ratio (3.5) and the taper angle (85°) has not yet been demonstrated. The main purpose of this study is to develop a etching process for Ru and RuO_2 with the high aspect ratios required for gigabit DRAM.

II. MECHANISM OF ANISOTROPIC RuO_2 ETCHING

The etching mechanisms of RuO_2 in O_2 plasmas are illustrated in Fig. 1. The Ru etching mechanism is believed to be similar to that of RuO_2. RuO_2 is etched by oxygen ion sputtering and by oxygen ion assisted etching through the formation of volatile RuO_3 and RuO_4. Sidewall coatings may develop through the redeposition of the sputtered component and the decomposition of the volatile compounds into solid Ru or RuO_2. The deposition of these reaction products on the sidewall decreases the taper angle of the etched profile and, thereby, limits the achievable aspect ratio. This effect can be minimized by reducing the partial pressure of the volatile etch products over the wafer, by increasing etching rate of the sidewall deposition with high density oxygen plasma, and by increasing exhaustivity of the reaction products with high gas flow rate and high speed pumping. We therefore implemented the RuO_2 and Ru etching processes in an inductively coupled plasma (ICP) etcher, which can generate a high density plasma with high gas flow rates at low pressure.

III. EXPERIMENTS

The ICP etcher used for RuO_2 and Ru etching experiments was as follows. It has a inductive coil of rectangular cross section placed on the top of a quart window. Radio frequency (rf) power with 13.56 MHz is applied to both the coil and a wafer electrode. Etching gases and productions are exhausted via 2000 little/s turbo molecular pump. The wafer is electrostatically chucked on the electrode.

Samples were prepared with three different layer sequences on 150 mm silicon wafers:

(a) Photoresist (2 μm thick)/plasma-tetraethylorthosilicate (P-TEOS) (200 nm)/RuO_2(250 nm)/Ru(50 nm)/TiN(80 nm)/Ti(50 nm). The CD of the resist pattern was 1 μm.
(b) Electron beam (EB) resist (300 nm thick)/P-TEOS(200 nm)/RuO_2(250 nm)/Ru(50 nm)/TiN(80 nm)/Ti(50 nm). The CD of the EB resist pattern was 0.14 μm.
(c) EB resist (300 nm thick)/P-TEOS(300 nm)/Ru(450 nm)/TiN(80 nm)/Ti(50 nm). The CD of the resist pattern was 0.1 μm.

The bottom layers of TiN/Ti were used for adhesion of RuO_2/Ru and Ru. The resist patterns on all the samples were transferred into the P-TEOS film by dry etching with a CHF_3/CF_4 plasma. The resulting P-TEOS masks were subsequently used to etch the RuO_2/Ru or Ru films in O_2 + 10% Cl_2. We first optimized the pressure and O_2 + 10% Cl_2 gas flow rate with the (a) samples under the condition of 500 W ICP source power and 200 W rf power. These optimal conditions were used to etch the (b) samples, which were then inspected to determine their anisotropy. Finally, anisotropic etching of Ru was examined using the (c) samples.

[a] Electronic mail: yunogami-takashi@nhmemory.co.jp
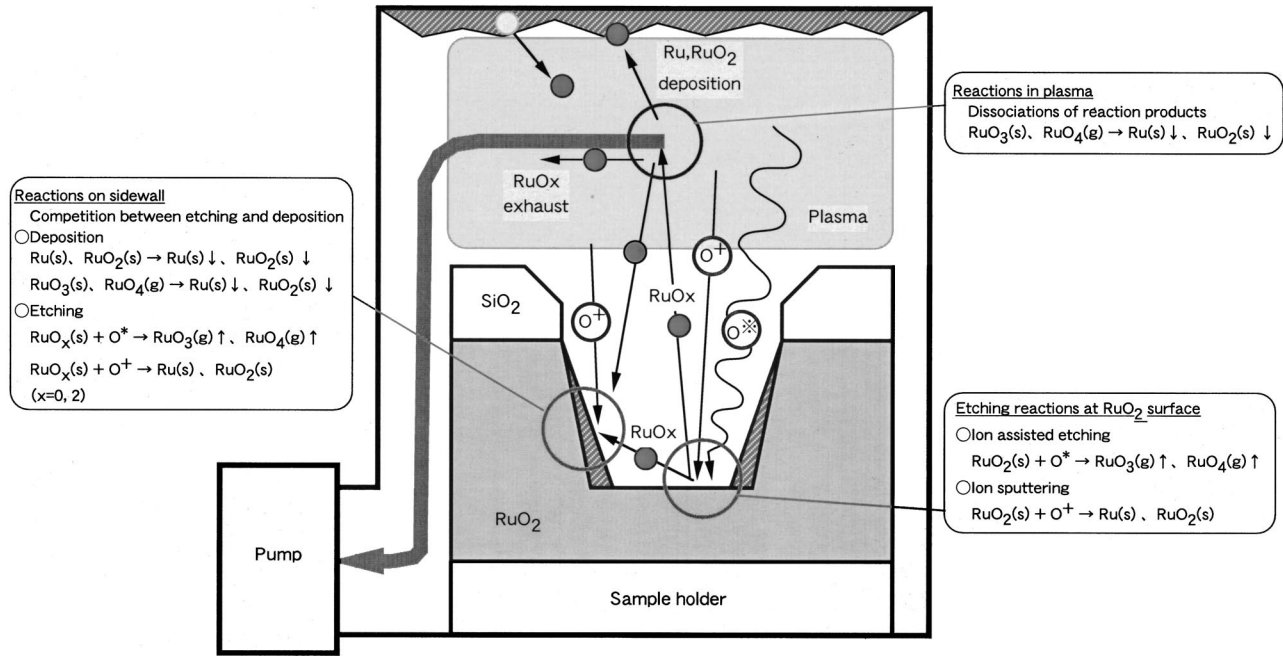
FIG. 1. Etching mechanism of RuO$_2$ with oxygen-based gas chemistry.

IV. RESULTS AND DISCUSSIONS

A. Optimization of process parameters

At first, pressure and O$_2$+10% Cl$_2$ gas flow rate were optimized for RuO$_2$/Ru etching using the (a) samples. Figures 2(A) and 3(A) show, respectively, scanning electron micrographs (SEMs) of the etched RuO$_2$/Ru structures and a summary of the etching characteristics (etch rate, taper angle, and facet width) as functions of pressure. As expected, taper angle increased as pressure decreased. However, reducing the pressure also increased the mask faceting, which leads to shoulder loss of the RuO$_2$. Based on these results, we chose 15 mTorr as the optimal pressure.

Figures 2(B) and 3(B) show, respectively, SEMs of the RuO$_2$/Ru etch profiles and a summary of etching characteristics (etch rate, taper angle, and facet width) as a function of O$_2$+10% Cl$_2$ gas flow rate. As again expected, taper angle

(A)
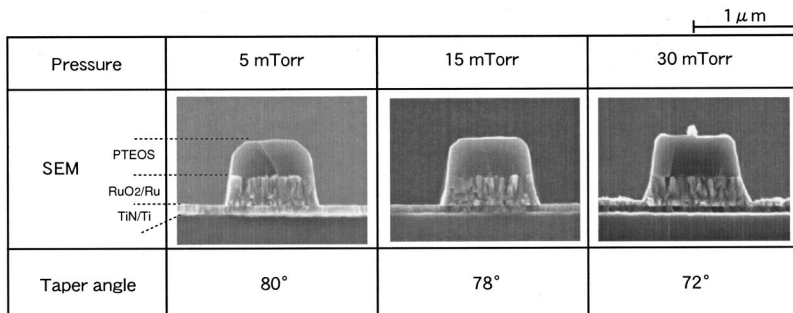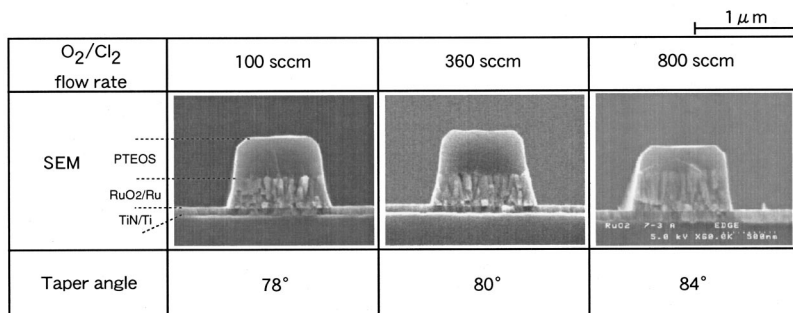
FIG. 2. RuO$_2$/Ru pattern profiles as a function of (A) pressure and (B) O$_2$+10% Cl$_2$ flow rate.

(B)
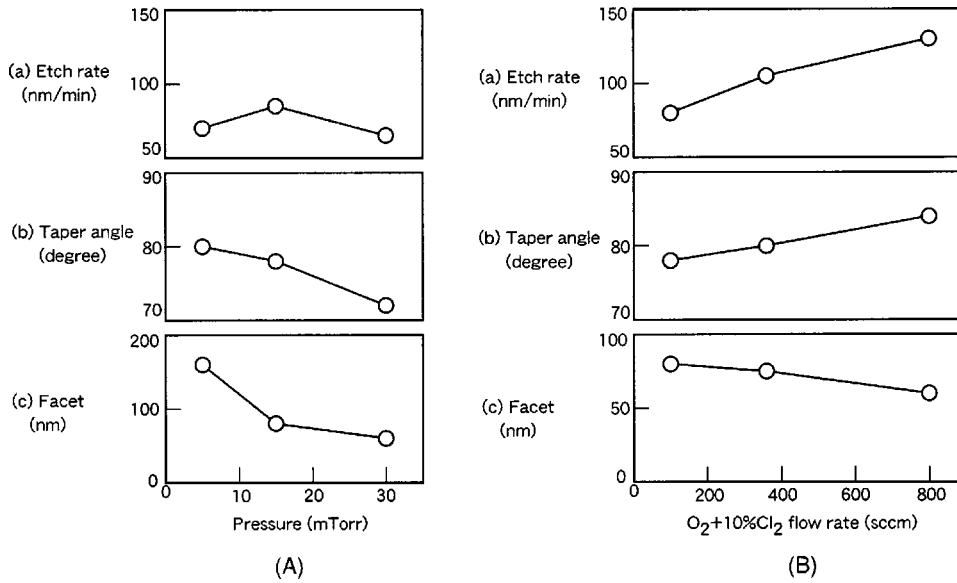
FIG. 3. RuO$_2$ etching characteristics as a function of (A) pressure and (B) O$_2$ + 10% Cl$_2$ flow rate.

increased with increasing gas flow rate. When the process conditions were 15 mTorr total pressure and 800 sccm gas flow rate, the taper angle of RuO$_2$/Ru became 84°, slightly lower than our goal of 85°. Since etch rate and faceting also improved with increasing gas flow rate, the optimal flow rate was chosen as the maximum (800 sccm) that could be achieved at the optimal pressure (15 mTorr).

B. Anisotropic etching of RuO$_2$/Ru

The high resolution RuO$_2$/Ru patterns of sample (b) were etched under the optimized conditions discussed earlier. The formation of the P-TEOS mask is shown in Fig. 4: (A) EB resist pattern with a CD of 0.14 μm and a thickness of 0.3 μm, (B) P-TEOS pattern with resist remaining (0.2 μm thick and 0.2 μm CD), and (C) the P-TEOS pattern after resist ashing. A small amount of resist residue remains after the ashing step. The 300-nm-thick RuO$_2$/Ru stack was then etched with the P-TEOS mask using the optimized conditions (15 mTorr pressure and 800 sccm O$_2$ + 10% Cl$_2$ flow rate). Figure 5 shows SEM photos of the RuO$_2$/Ru pattern as a function of percent overetch (OE%), defined as the total etching time less the time required to etch just though the RuO$_2$/Ru stack expressed as a percentage of the time to etch the stack. The taper angle increases during the overetch period (e.g., with OE%) because RuO$_x$ ($x = 0 - 4$) no longer evolves from the bottom of the trench but the sidewalls continue to etch. Figure 6 shows a RuO$_2$/Ru pattern with OE% = 100 that has an almost perpendicular taper angle of 89°. Moreover, the CD of the RuO$_2$/Ru stack was 0.22 μm, corresponding to a CD gain of 20 nm relative to the TEOS mask. This is sufficiently small for current design rules.

C. Anisotropic Ru etching

Finally, Fig. 7 shows a 450-nm-thick Ru film [sample (c)] etched with a P-TEOS mask (0.3 μm thick and 0.1 μm CD) under the same conditions discussed earlier for RuO$_2$/Ru.
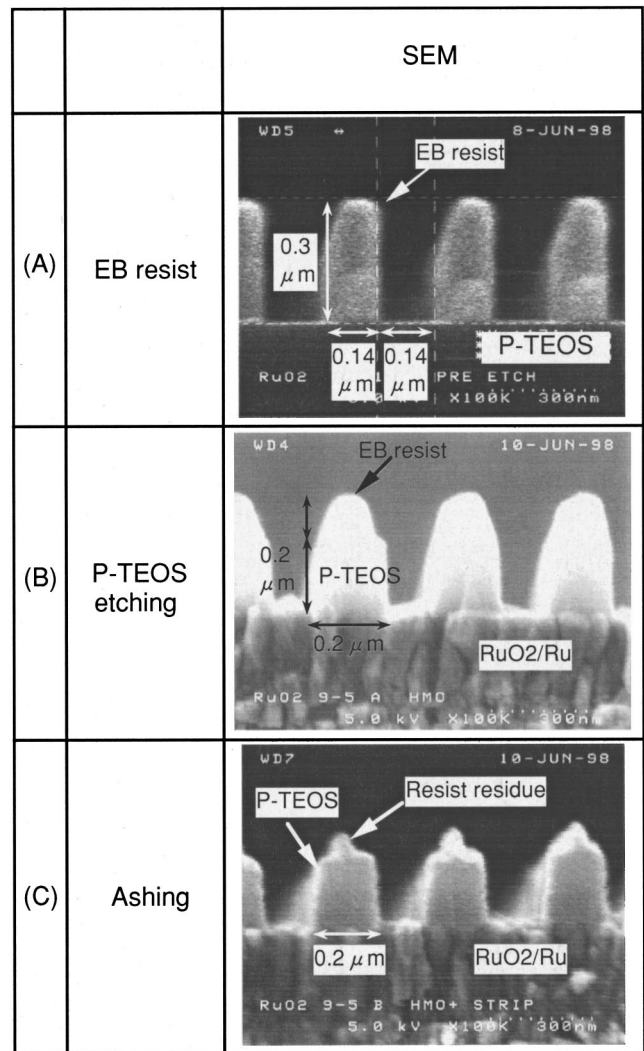
FIG. 4. P-TEOS mask formation. (A) EB resist pattern, (B) P-TEOS etching, and (C) ashing.

FIG. 5. Taper angle of RuO_2/Ru pattern as a function of overetch percentage.

The resulting Ru pattern is 0.45 μm in height and 0.1 μm wide, corresponding to an aspect ratio of 4.5. The taper angle was 89°, and the CD gain was almost zero.
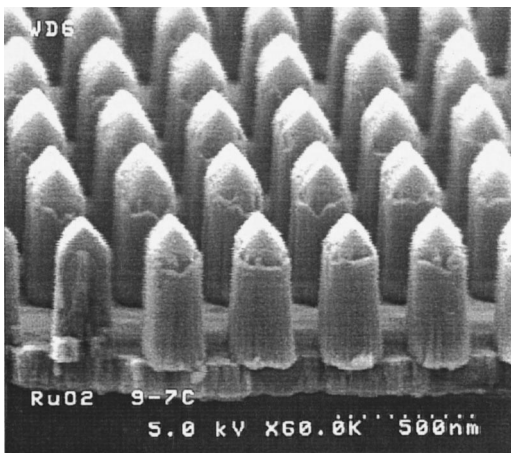
FIG. 6. High aspect ratio RuO_2/Ru profile.
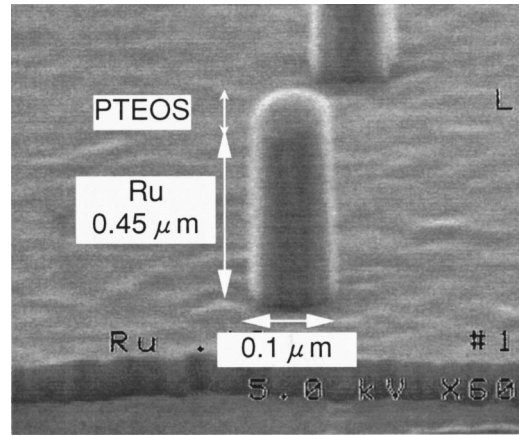
FIG. 7. High aspect ratio Ru profile.

V. CONCLUSIONS

Anisotropic etching technology for RuO_2 and Ru has been developed using a high density $O_2 + 10\%$ Cl_2 plasma in an ICP etching system. The taper angle for RuO_2/Ru increased with decreasing pressure, with increasing $O_2 + 10\%$ Cl_2 flow rate and with increasing overetch time. Using a low pressure, a high gas flow rate and 100% over etch time resulting in a 0.3-μm thick RuO_2/Ru pattern with 0.2 μm CD and a taper angle of 89°. A 0.45-μm-thick Ru pattern with 0.1 μm CD and a taper angle of 89° was formed using the same etching process. Thus, we have demonstrated a process suitable for etching the electrodes of high-dielectric constant capacitors in gigabit DRAM manufacturing.

ACKNOWLEDGMENTS

[1] S. Yamamichi, K. Takemura, T. Sakura, H. Watanabe, H. Ono, K. Tokashiki, E. Ikawa, and Y. Miyasaka, *Proceedings of the 1994 IEEE 9th Symposium on the Application of Ferroelectrics* (IEEE, University Park, PA, 1994).
[2] H. Yamaguchi, S. Matsubara, K. Takemura, and Y. Miyasaka, *Proceedings of the 1992 IEEE 8th Symposium on the Application of Ferroelectrics* (IEEE, Piscataway, NJ, 1992), p. 258.
[3] W. J. Yoo, J. H. Hahm, C. S. Hwang, S. O. Park, Y. B. Koh, and M. Y. Lee, Proceedings of the Dry Process Symposium (1995), p. 191.
[4] T. Yunogami and T. Kumihashi, Jpn. J. Appl. Phys., Part 1 **37**, 6934 (1998).
[5] *Handbook of Chemical and Physics*, 76th ed., edited by D. R. Lide (CRC Press, Boston, 1995).
[6] K. Tokashiki, K. Sato, K. Takemura, S. Yamamichi, P. Y. Lesaicherre, H. Miyamoto, E. Ikawa, and Y. Miyasaka, Proceedings of the Dry Process Symposium (1994), p. 73.
[7] K. Nakamura, T. Shibano, and T. Oomori, Proceedings of the Dry Process Symposium (1997), p. 217.
[8] W. E. Bell and M. Tagami, J. Phys. Chem. **67**, 2432 (1963).
[9] E. J. Lee, J. W. Kim, and W. J. Lee, Jpn. J. Appl. Phys., Part 1 **37**, 2634 (1998).